

Dynamic Contact Behavior of a Golf Ball during Oblique Impact: Effect of Friction between the Ball and Target

K. Arakawa · T. Mada · H. Komatsu · T. Shimizu ·
M. Satou · K. Takehara · G. Etoh

Received: 11 June 2006 / Accepted: 23 October 2006 / Published online: 24 January 2007
© Society for Experimental Mechanics 2007

Abstract The oblique impact between a golf ball and a polymethyl methacrylate (PMMA) target with smooth transparent surfaces was studied using a high-speed video camera. Video images of the impact were recorded from the backside of the target and were used to determine the contact time, contact area, and the displacement and rotation of the ball along the target. The average tangential and angular velocities were determined as functions of the inbound ball velocity. As the inbound ball velocity increased, the contact area and average tangential and angular velocities also increased while the contact time decreased. An oiled PMMA target was used to study the effect of reduced friction between the ball and target. The results were compared with earlier data for a steel target with relatively rough surfaces. The contact area and time were unaffected by friction, but the average tangential velocity increased while the average angular velocity decreased as the friction decreased.

Keywords Golf ball · Oblique impact · Friction effect · PMMA target · High-speed video camera · Inbound velocity ·

Contact time and area · Displacement and rotation · Tangential and angular velocity · Steel target

Introduction

Many researchers have studied the impact behavior of a golf ball to determine the dynamic contact force and time, the coefficient of restitution, and spin rate of the ball as a function of the impact velocity [1–10]. The contact force and spin rate increase significantly with velocity while the contact time and coefficient of restitution gradually decrease. The mechanism of such impact behavior, however, is not well understood. In theoretical analyses [11–15], a rigid body model for oblique impacts has been used to suggest that friction between the ball and target gradually reduces the tangential ball velocity along the target and gradually increases the angular ball velocity. Although friction plays an important role in the dynamic contact behavior, the mechanism again has not been demonstrated experimentally.

We previously examined the dynamic contact behavior of a golf ball during an oblique impact with a rigid steel target [16]. The ball was launched horizontally at velocities between 10 and 60 m/s using an air gun, and struck the target at an oblique angle of 30°. The dynamic contact behavior was photographed using a high-speed video camera [17]. Since this camera was capable of recording 100 frames at a maximum speed of 1×10^6 frames/s, it permitted quantitative measurements of the dynamic contact behavior. We evaluated the inbound and rebound ball velocities and angles, contact time, and average tangential and angular velocities. When the results from a rigid body model were compared to the experimental data, the model had predicted the experimental data to some extent.

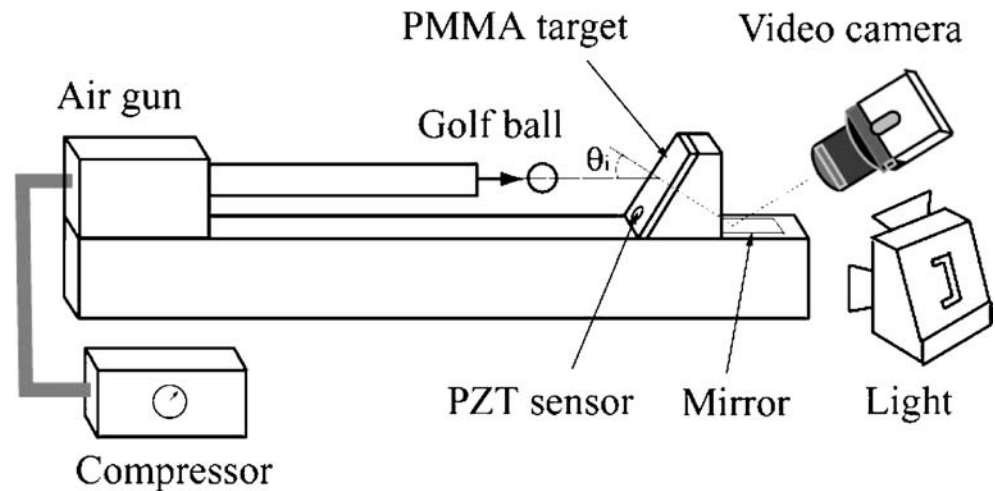
K. Arakawa (✉, SEM member) · T. Mada · H. Komatsu
Research Institute for Applied Mechanics, Kyushu University,
6-1 Kasuga-koen, Kasuga-shi, 816-8580 Fukuoka, Japan
e-mail: k.arakaw@riam.kyushu-u.ac.jp

T. Shimizu
Maruman & Co., Ltd., Tokyo, Japan

M. Satou
Apen Engineering Office, Tokyo, Japan

K. Takehara · G. Etoh
School of Science and Engineering, Kinki University,
Osaka, Japan

Fig. 1 Schematic diagram of the experimental apparatus



The present study examined oblique impacts between a golf ball and a polymethyl methacrylate (PMMA) target with smooth transparent surfaces to investigate the effect of friction. High-speed video images were recorded from the backside of the target and used to determine the contact time, contact area, and the ball center, contact center, and initial contact point displacements. The average tangential and angular ball velocities along the target were then calculated. An oiled PMMA target was used to study the effect of reduced friction between the ball and target. The results were correlated with earlier data for a steel target having a relatively rough surface [16], and we discuss the findings in this report.

Experimental Methods

The experiment was performed using the apparatus illustrated in Fig. 1. A golf ball was launched using an air gun so that it obliquely struck a PMMA target clamped to a rigid steel frame. The target, which had smooth transparent surfaces, was $130 \times 170 \text{ mm}^2$ and 20 mm thick; its surface had been degreased with alcohol. An oiled PMMA target was also used to reduce the friction between the ball and target. The distance from the gun muzzle to the target was 450 mm and the inbound ball velocity was varied between 15 and 60 m/s. The velocity was determined by measuring the time interval between two laser beams intercepted by the inbound ball. The ball struck the target at a nominal angle of 30° to the normal and rebounded in the same vertical plane.

The dynamic contact behavior was recorded using a high-speed video camera (HPV-1; Shimadzu Co.) [17]. The camera was triggered using a piezoelectric sensor when the inbound ball hit the target. The high-speed images were recorded from the backside of the PMMA target using a

mirror (see Fig. 1). The images were recorded using a framing interval of $10 \mu\text{s}$ and saved as a bitmap having 312×260 pixels. Two-piece golf balls (Pinnacle; Acushnet, Brockton, MA, USA) were used in this study. The diameter and mass of the balls were 42.6 mm and 46 g, respectively. All of the experiments were conducted using new 90-compression balls and new targets in order to avoid changes in surface roughness due to impact.

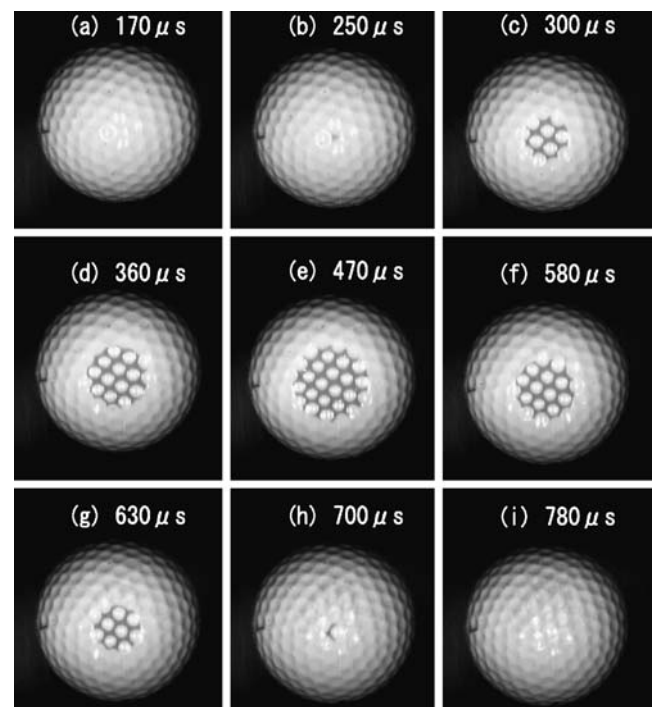


Fig. 2 High-speed video images of the golf ball during the oblique impact with a transparent PMMA target ($v_i=31.5 \text{ m/s}$, $\Delta t=10 \mu\text{s}/\text{frame}$)

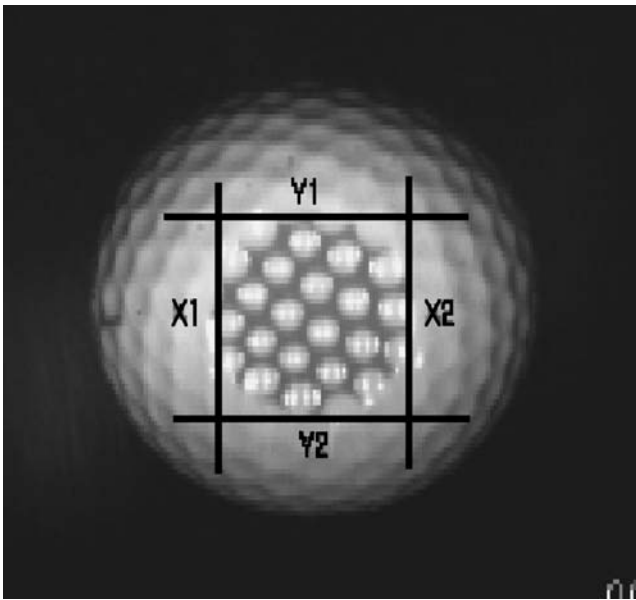


Fig. 3 Measurement technique for the contact surface area

Results and Discussion

High-speed video images during impact

Figure 2 shows nine images combined to illustrate the dynamic contact behavior of the ball, where (a) is an image recorded before impact, (b) shows the initial contact with the target, (c)–(g) show the compression and restitution phases, (h) indicates the final contact prior to rebounding, and (i) shows the ball after the impact. Several interesting observations were made: the contact area became dark due to diffused reflection, the contact area increased in the early stages of the impact and then decreased in the later stages, the dimples on the ball surface barely contacted the target, and the ball moved along the target during the impact. The contact time, contact area, and average angular and tangential ball velocities along the target were measured using these images.

Fig. 4 Ball cross section A_b , contact area A_c , and noncontact area A_d

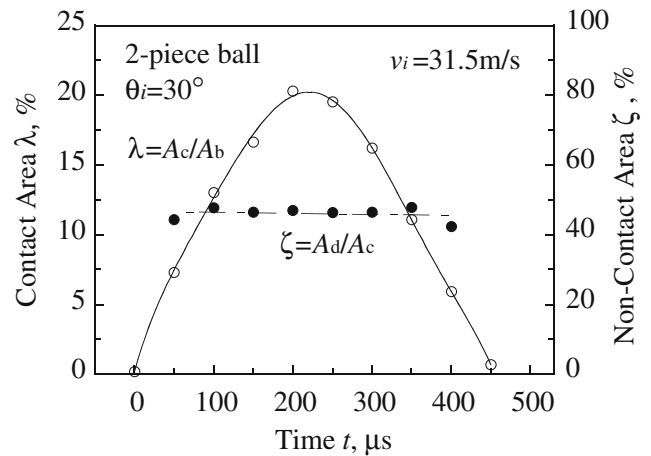
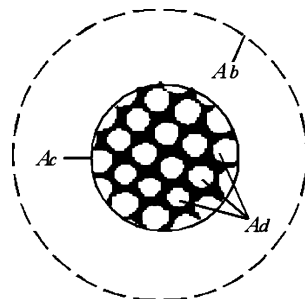


Fig. 5 Values of the contact area $\lambda(=A_c/A_b)$ and noncontact area $\zeta(=A_d/A_c)$ as a function of time t

Contact area

The contact area between the ball and target during impact was measured as indicated in Fig. 3. The X – Y coordinates of the contact area, i.e., (X_1, X_2) and (Y_1, Y_2) , were determined, and then the contact area A_c was calculated using following equation (see Fig. 4):

$$A_c = \pi(X_2 - X_1)(Y_2 - Y_1)/4. \tag{1}$$

The following parameters were introduced:

$$\lambda = A_c/A_b, \zeta = A_d/A_c, \tag{2}$$

where A_b and A_d are the cross section of the ball and the total noncontact area due to the dimples, respectively. The cross section of the ball was determined by reversing the gradation of the image and clarifying the outline of the ball as indicated by the dashed line in Fig. 4. The noncontact area A_d was determined as follows. First, images of the area A_c were digitized. Then, the contact and noncontact areas

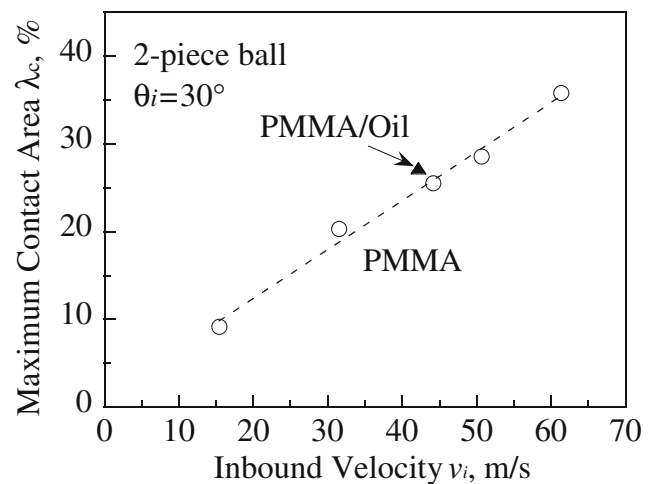


Fig. 6 Relationship between the maximum contact area λ_c and the inbound ball velocity v_i

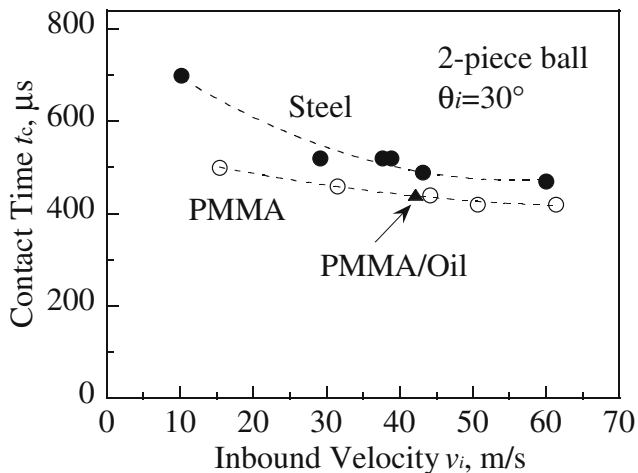


Fig. 7 Relationship between the contact time t_c and the inbound ball velocity v_i

were shaded black and white, respectively. Finally, the total noncontact area A_d was evaluated from the ratio of the white pixels in the histogram.

Figure 5 shows the contact area λ and the noncontact area ζ as a function of time t , where the initiation of the impact is denoted by $t=0$. As plotted in the figure, λ increased in the early stages of the impact and then decreased in the later stages. The maximum value of λ was 20% at $t=220 \mu\text{s}$ for an inbound ball velocity $v_i=31.5 \text{ m/s}$. The λ - t curve was not symmetric: a slight convex slope in the compression phase and a concave slope in the restitution phase were observed. Similar results have also been reported in measurements of impact load [1, 7] and compression ratio [16] due to the viscoelastic deformation of the ball during impact. In contrast, ζ remained almost constant with t at 46%. This implies that the dimples barely contacted the target during the impact.

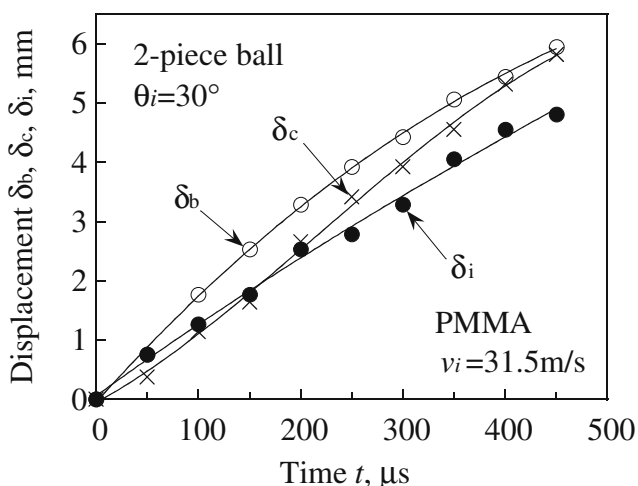


Fig. 8 Ball center displacement δ_b , contact center displacement δ_c , and initial contact point displacement δ_i as a function of time t

Figure 6 gives the maximum contact area λ_c versus the inbound ball velocity v_i , where the circles and triangle correspond to the degreased target and the oiled target, respectively. As indicated by the figure, λ_c increased almost linearly with v_i and was not affected by the oil. This suggests that the contact area was not dependent on the friction between the ball and target, and that it was influenced only by the inbound ball velocity or the compressive force between the ball and target.

Contact time

The contact time t_c between the ball and PMMA target was determined from the initial and final contact images (see Fig. 2). The results obtained from single shots are plotted in Fig. 7 as a function of the inbound ball velocity v_i , where t_c values for the oiled PMMA target and the steel target studied previously [16] are also indicated. The oil had no influence on t_c ; almost the same values were determined for the PMMA and oiled targets, similar to the findings for contact area λ_c . In contrast, the target material had a significant influence on the results. As shown in the figure, t_c decreased with v_i for the PMMA and steel targets, but the PMMA target had much smaller t_c values for a given v_i . This difference is not expected from the Hertz law which assumes the theory elasticity and small deformation [18]. Hence, the reason for this is not well understood, but could be related to the material properties such as the elastic modulus and density of the ball and target or the impedance mismatch between the two materials. Higher modulus and density of the steel target could result in larger ball deformation and contact time for a given v_i . Also, a larger impedance mismatch between the ball and the steel target could result in the same effect, since the energy loss due to the elastic wave propagation from the ball into the target could decrease. It should be noted that the differences between the contact times measured for the steel and PMMA targets were much larger than that of the maximum measurement error ($20 \mu\text{s}$) due to the framing interval ($10 \mu\text{s}$).

Ball center, contact center, and initial contact point displacements

To study the tangential and angular ball velocities, we measured the deformation of the ball on the target with the assumption that it was much smaller than the distance between the target and camera (see Fig. 1). The initial contact point was determined as follows: First, the image where contact initiated between ball and the target was selected [see Fig. 2(b)]. Second, that image was enlarged and the center of the contact area was determined as shown in Fig. 3. Finally, the center of the contact area was used as

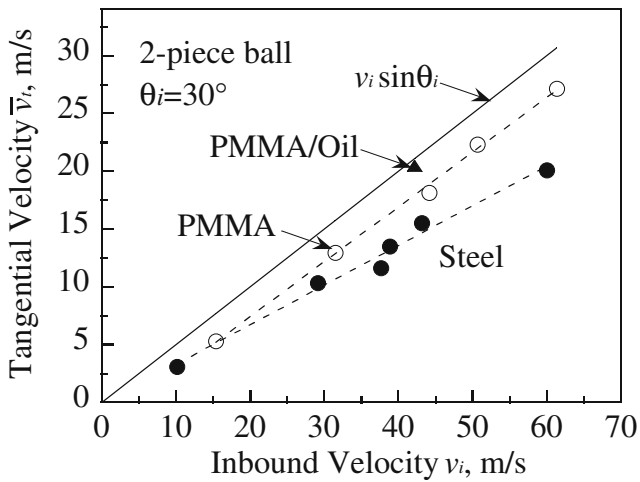


Fig. 9 Relationship between the average tangential ball velocity \bar{v}_t as a function of the inbound ball velocity v_i

the initial contact point and the displacement of that point was measured as a function of time during impact. A similar procedure was used to determine the ball center and the contact center displacements. The results are shown in Fig. 8, where the ball center, contact center, and initial contact point displacements are denoted as δ_b , δ_c , and δ_i , respectively (see Figs. 2 and 4). Although they increased with time t , as expected, several interesting observations were made. The difference between δ_b and δ_c , *i.e.*, $\delta_{bc} = (\delta_b - \delta_c)$, increased in the early stages of the impact and then decreased in the later stages. This tendency was similar to the increasing and decreasing behavior of the contact area λ (see Fig. 5). Hence, δ_{bc} might be related to the shear deformation of the ball induced by the inertia and friction along the target. In contrast, the difference between δ_b and δ_i , *i.e.*, $\delta_{bi} = (\delta_b - \delta_i)$, increased with time t

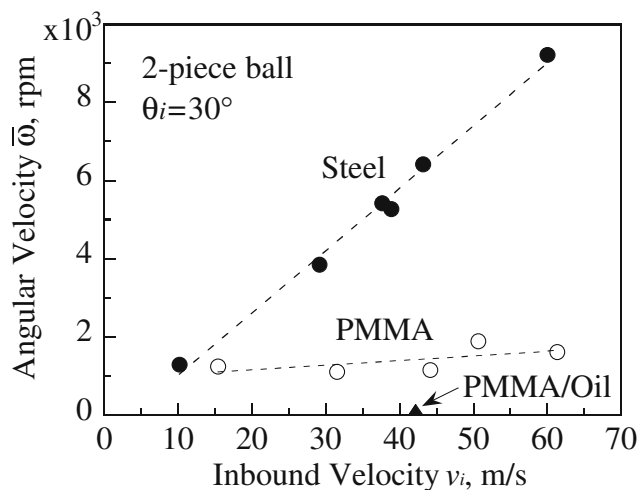


Fig. 10 Relationship between the average angular ball velocity $\bar{\omega}$ as a function of the inbound ball velocity v_i

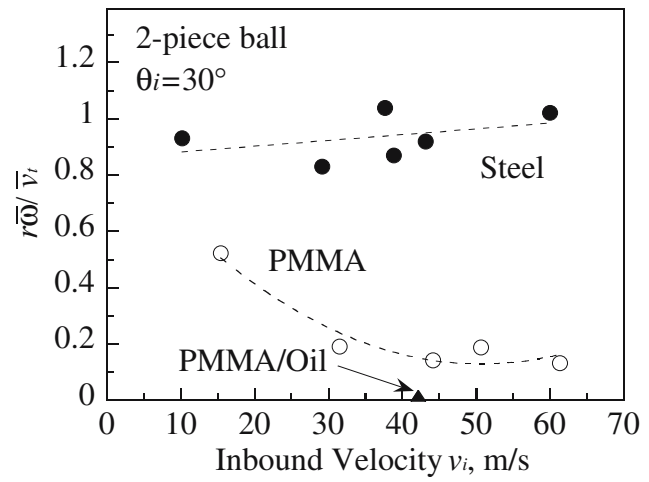


Fig. 11 Relationship between the values of $r\bar{\omega}/\bar{v}_t$ as a function of the inbound ball velocity v_i

throughout the impact, whereas δ_{bi} should remain constant if no rotation occurs in the ball. Hence, the ball slid and rotated along the target.

Average tangential and angular ball velocities

Using the ball center displacement δ_b and initial contact point displacement δ_i , the average tangential velocity \bar{v}_t and average angular velocity $\bar{\omega}$ along the target were determined as follows:

$$\bar{v}_t = \delta_b/t_c, \quad \bar{\omega} = \theta_c/t_c = \delta_{bi}/r t_c = (\delta_b - \delta_i)/r t_c, \quad (3)$$

where t_c , θ_c , and r are the contact time, rotation angle, and radius of the ball, respectively. Here, we assumed that δ_{bi} was very small compared to r , and r was constant during impact.

Figure 9 shows the values of \bar{v}_t for the degreased PMMA target, oiled PMMA target, and steel target, where $v_i \sin\theta_i$ is the initial tangential velocity with zero friction. As shown in the figure, \bar{v}_t increased almost linearly with the inbound ball velocity v_i . However, the effect of friction was observed since the oiled PMMA target gave the largest value of \bar{v}_t for a given v_i , followed by the degreased PMMA target and the steel target. This implies that \bar{v}_t increased as the friction decreased.

The values of $\bar{\omega}$ are plotted in Fig. 10 as a function of v_i . The target material had a significant effect on the results. As the figure illustrates, $\bar{\omega}$ for the steel target increased almost linearly up to 9,216 rpm for $v_i=60$ m/s. However, it dropped sharply to 1,620 rpm for the PMMA target and it was nearly zero for the oiled target, suggesting that $\bar{\omega}$ decreased as the friction decreased.

To study the effect of friction in more detail, the values of $r\bar{\omega}/\bar{v}_t$ were plotted as a function of v_i , assuming the ball radius r to be constant during impact (Fig. 11). As shown in

the figure, the value of $r\bar{\omega}/\bar{v}_t$ for the PMMA target decreased from 0.52 to 0.13 as v_i increased from 15 to 61 m/s and was almost zero for the oiled target. In contrast, the steel target gave much larger values than that of the PMMA target. This suggests that the angular velocity of the ball was fully developed during impact with the rough steel target. Also, the impact of the ball on the PMMA target with a smooth surface yielded a much smaller angular velocity than expected. The friction effect was almost negligible on the very smooth oiled PMMA surface, implying that friction plays an important role in developing angular velocity during impact.

Conclusions

We conducted impact tests of a golf ball and a PMMA target with smooth transparent surfaces at an oblique impact angle of 30°. High-speed video images were recorded during the impact from the backside of the target. The contact images between the ball and target were used to determine the contact time, contact area, and the ball center, contact center, and initial contact point displacements during the impact. The average tangential and angular velocities were then calculated. An oiled PMMA target was also used to study the effect of reduced friction between the ball and target. The results were compared with earlier data for a rigid steel target with relatively rough surfaces. For an inbound ball velocity ranging from 15 to 61 m/s, the following results were obtained.

- (1) As the inbound ball velocity increased, the contact area increased while the contact time decreased.
- (2) A large friction effect was not observed for the contact time and area.
- (3) As the inbound ball velocity increased, the average tangential and angular velocities increased for the PMMA and steel targets.
- (4) For a given inbound velocity, the oiled PMMA target resulted in the largest tangential velocity of the ball, followed by that of the degreased PMMA target and then that of the steel target.
- (5) The average angular velocity of the ball after impact with the steel target was much larger than that of the degreased PMMA target and was nearly zero for the oiled PMMA target.

References

1. Ujihashi S, Hirahara Y, Adachi T, Matsumoto H (1994) Measurement and evaluation of restitution characteristic of golf balls (in Japanese). *Trans Jpn Soc Mech Eng C* 60(577):3150–3156.
2. Ekstrom EA (1998) Experimental determination of golf ball coefficients of sliding friction. *Science and golf III. Proc. of the World Science Congress of Golf*, Chapter 64, pp 510–518.
3. Johnson SH, Ekstrom EA (1998) Experimental study of golf ball oblique impact. *Science and golf III. Proc. of the World Science Congress of Golf*, Chapter 65, pp 519–525.
4. Hocknell A, Jones R, Rothberg S (1996) Experimental analysis of impacts with large elastic deformation: I. Linear motion. *Meas Sci Technol* 7:1247–1254.
5. Chou PC, Yang LJ (1994) Contact forces, coefficient of restitution, and spin rate of golf ball impact. *Science and golf II. Proc. of the World Scientific Congress of Golf*, pp 297–301.
6. Yokoyama T, Yamada Y (1999) Measurement of restitution characteristics of golf balls, effect of impact velocity and golf club head materials (in Japanese). *Prepr of Jpn Soci Mech Eng, Symp on Sport Engineering* 198–202.
7. Yokoyama T, Yamada Y (2000) A relation between compression number and coefficient of restitution of golf balls (in Japanese). *Prepr of Jpn Soci Mech Eng, Symp on Sport Engineering* 170–174.
8. Kurokawa T, Urabe D (2000) Impact properties of golf ball II (in Japanese). *Prepr of Jpn Soci Mech Eng, Symp on Sport Engineering* 86–90.
9. Komatsu H, Simizu T, Mada T, Satou M, Arakawa K (2002) Dynamic contact time measurements on impacted golf balls (in Japanese). *J JSEM* 2(3):33–38.
10. Roberts JR, Jones R, Rothberg SJ (2001) Measurement of contact time in short duration sports ball impacts: an experimental method and correlation with the perceptions of elite golfers. *Sports Eng* 4:191–203.
11. Daish CB (1972) *The physics of ball games*. Hazell Watson & Viney Ltd, Aylesbury Bucks, UK, pp 161–167.
12. Kawamura R (1996) *Science of golf* (in Japanese). *Jpn J Golf Sci* 9(2):56–60.
13. Iwatsubo T, Nakagawa N, Akao M, Mominaga I, Yamaguchi T (1990) Optimum design of a golf club head (in Japanese). *Trans Jpn Soc Mech Eng C* 56(524):203–209.
14. Cochran AJ (1998) Club face flexibility and coefficient of restitution. *Science and golf III. Proc. of the World Science Congress of Golf*, Chapter 61, pp 486–492.
15. Simizu T, Komatsu H, Mada T, Takahashi K, Satou M (1998) Analysis of the spinning mechanism of golfball using the “s Parameter” and its experimental certification (in Japanese). *Trans Jpn Soc Mech Eng C* 64(623):3150–3156.
16. Arakawa K, Mada T, Komatsu H, Simizu T, Satou M, Takehara K, Etoh G (2006) Dynamic contact behavior of a golf ball during oblique impact. *Exp Mech* 46:691–697
17. Maruno H, Takubo K, Tominaga H, Soya H, Kondo Y, Takehara K, Etoh G (2001) Development of high-speed video camera with ISIS-CCD. *Japan Congress on High Speed Photography and Photonics*, pp 1–4.
18. Goldsmith W (1960) *Impact: the theory and physical behaviour of colliding solids*. Edward Arnold (Publishers) Ltd., London, UK, pp 82–90.